Video Article

Synthesis and Testing of Supported Pt-Cu Solid Solution Nanoparticle Catalysts for Propane Dehydrogenation

Zixue Ma[1], Zhenwei Wu[1], Jeffrey T. Miller[1]

[1]Davidson School of Chemical Engineering, Purdue University

Correspondence to: Jeffrey T. Miller at jeffrey-t-miller@purdue.edu

URL: https://www.jove.com/video/56040
DOI: doi:10.3791/56040

Keywords: Chemistry, Issue 125, Bimetallic catalysts, nanoparticles, propane dehydrogenation, Pt-Cu, solid solution, *in situ* X-ray diffraction, *in situ* X-ray absorption spectroscopy

Date Published: 7/18/2017

Citation: Ma, Z., Wu, Z., Miller, J.T. Synthesis and Testing of Supported Pt-Cu Solid Solution Nanoparticle Catalysts for Propane Dehydrogenation. *J. Vis. Exp.* (125), e56040, doi:10.3791/56040 (2017).

Abstract

A convenient method for the synthesis of bimetallic Pt-Cu catalysts and performance tests for propane dehydrogenation and characterization are demonstrated here. The catalyst forms a substitutional solid solution structure, with a small and uniform particle size around 2 nm. This is realized by careful control over the impregnation, calcination, and reduction steps during catalyst preparation and is identified by advanced *in situ* synchrotron techniques. The catalyst propane dehydrogenation performance continuously improves with increasing Cu:Pt atomic ratio.

Video Link

The video component of this article can be found at https://www.jove.com/video/56040/

Introduction

Propane dehydrogenation (PDH) is a key processing step in the production of propylene, taking advantage of shale gas, the fastest growing source of gas in the country[1]. This reaction breaks two C-H bonds in a propane molecule to form one propylene and molecular hydrogen. Noble metal catalysts, including Pd nanoparticles, exhibit poor selectivity for PDH, breaking the C-C bond to produce methane with a high yield, with the concomitant production of coke, leading to catalyst deactivation. Recent reports showed that selective PDH catalysts could be obtained by the addition of promoters like Zn or In to Pd[2,3,4]. The promoted catalysts are near 100% selective to PDH, as opposed to less than 50% for monometallic Pd nanoparticles of the same size. The great improvement in selectivity was attributed to the formation of PdZn or PdIn intermetallic compound (IMC) structures on the catalyst surface. The ordered array of two different types of atoms in the IMCs geometrically isolated the Pd active sites with non-catalytic Zn or In atoms, which turned off the side reactions catalyzed by an ensemble (group) of neighboring Pd active sites.

Platinum has the highest intrinsic selectivity among noble metals for propane dehydrogenation, but it is still not satisfactory for commercial use[1]. Typically, Sn, Zn, In, or Ga is added as promoter for Pt[5,6,7,8,9,10,11,12,13]. Based on the idea that geometric active site isolation contributes to high selectivity, any non-catalytic element forming an alloy structure with Pt, such as Cu, should also potentially promote catalyst performance[14]. Several previous studies suggested that the addition of Cu indeed improved the PDH selectivity of Pt catalysts[15,16,17,18]. Nevertheless, no direct evidence has been reported to determine whether Pt and Cu form bimetallic nanoparticles or ordered structures, which is crucial to understanding the promotional effect of Cu. In the binary phase diagram of Pt-Cu, two different structure types are possible over a wide composition range[16,18]: intermetallic compound, in which Pt and Cu each occupy specific crystal sites, and solid solution, in which Cu randomly substitutes in the Pt lattice. IMCs form at low temperature and transform into solid solution at around 600 - 800 °C for bulk materials[14]. This transformation temperature may be lower for nanoparticles, near the reaction temperature of PDH (*i.e.* 550 °C). Therefore, it is essential to investigate the atomic order of Pt-Cu under reaction conditions. For supported nanoparticles with small particle sizes, it is very challenging to obtain meaningful structural information using laboratory instruments[19]. The limited repetition of unit cells leads to very broad diffraction peaks with very low intensities. Because of the high fraction of surface atoms in nanoparticles 1 - 3 nm in size, which are oxidized in air, diffraction must be collected *in situ* using high-flux X-ray, typically available with synchrotron techniques.

The previously reported Pt-Cu PDH catalysts were all larger than 5 nm in size[15,16,17,18]. However, for noble metal nanoparticle catalysts, there is always a strong desire to maximize catalytic activity per unit cost by synthesizing catalysts with high dispersions (typically around or less than 2 nm in size)[19]. Though the preparation of bimetallic nanoparticles of this size is possible by standard impregnation methods, rational control over the procedures is necessary. The metal precursors, pH of the impregnating solution, and support type need to be controlled to optimize the anchoring of the metal species onto high-surface area supports. The subsequent calcination and reduction heat treatments should also be carefully controlled to suppress the growth of the metallic nanoparticles.

This article covers the protocol for the synthesis of supported 2 nm Pt-Cu bimetallic nanoparticle catalysts and for the testing of their propane dehydrogenation performance. The structure of the catalysts is investigated by Scanning Transmission Electron Microscopy (STEM), *in situ*

synchrotron X-ray Absorption Spectroscopy (XAS), and *in situ* synchrotron X-ray diffraction (XRD), which help elucidate the improved catalyst performance upon the introduction of Cu.

Protocol

1. Synthesis of Supported 2 nm Pt-Cu Bimetallic Nanoparticle Catalysts

1. **Preparation of metal precursor solution**
    1. Dissolve 0.125 g of copper nitrate trihydrate ($Cu(NO_3)_2 \cdot 3H_2O$) in 1 mL of water to achieve a sky blue solution.
    Caution: Use protective gloves when handling chemicals.
    2. Add ammonia dropwise to the copper nitrate solution, forming dark blue precipitates of copper hydroxide.
    Caution: Use a fume hood for handling bases and volatile chemicals.
    3. Keep adding ammonia until the dark blue precipitates dissolve to form a dark blue solution and the pH >10.
    4. Add 0.198 g of tetraammineplatinum nitrate ($(NH_3)_4Pt(NO_3)_2$) to the solution and additional water so that the total volume of the solution is 3.5 mL. Add additional ammonia if necessary to keep the pH of the solution greater than 10.
    5. Heat the solution to 70 °C until all the tetraammineplatinum nitrate salts are dissolved in the solution. Allow the solution cool to RT.

2. **Co-impregnation of metal precursor solution**
    1. Prior to catalyst preparation, determine the impregnating pore volume of the silica support. Carefully weigh approximately 5 g of dry silica into a weighting dish. While mixing, add H_2O dropwise until the silica is completely wet, but with no excess solution. Reweigh the wet silica. Divide the grams of added water by the grams of sample to calculate the pore volume.
    2. Add the dissolved metal precursor solution a few drops at a time to 5 g of high-porous silica (SiO_2) in a ceramic evaporating dish and stir gently to break up the particles that stick together to achieve a homogeneous distribution of the solution.
    NOTE: The white silica will turn dark blue once it adsorbs all 3.5 mL of metal precursor solution.
        1. Make sure that the texture of the silica particles remains like that of dry sand. Avoid the accumulation of excess solution during impregnation.
    3. Place the impregnated Pt-0.7Cu/SiO_2 catalyst precursor into a drying oven and dry it at 125 °C O/N.

3. **Calcination and reduction**
    1. Calcine the catalyst in a furnace at 250 °C with a 5 °C/min ramp rate in air for 3 h.
    NOTE: Calcination at higher temperatures generally leads to larger Pt nanoparticles.
    2. Place a 2 cm layer of quartz wool in the middle of a 1" quartz tube reactor and load the calcined Pt-0.7Cu/SiO_2 catalyst into the tube through a plastic funnel. Place the tube in a clamshell temperature-programmed furnace.
    3. After purging the tube with N_2 for 5 min at RT, start to flow H_2 (at RT) at the same flow rate as N_2 (100 ccm) to reduce the Pt-0.7Cu/SiO_2 catalyst.
    4. Increase the temperature to 150 °C with a 5 °C/min ramp rate and hold for 5 min.
    5. Start slow ramping the temperature at a rate of 2.5 °C/min to 250 °C. Hold the temperature for 15 min at every 25 °C.
    NOTE: Other metals may require lower or higher temperatures of reduction. The exact temperature can generally be determined by examining color changes of the catalyst (*e.g.,* from blue to black) for Pt-Cu.
    6. Ramp to 550 °C (or the reaction temperature, if higher) at 10 °C/min and stay for 30 min to complete the reduction. Purge with N_2 and cool to room temperature.
    7. Unload the Pt-0.7Cu/SiO2 catalysts and store in a vial for future use.
    NOTE: Repeat similar synthesis procedures using different amount of $Cu(NO_3)_2 \cdot 3H_2O$ and $(NH_3)_4Pt(NO_3)_2$ to prepare the other Pt-X Cu/SiO_2 catalysts (X = 0.7, 2.3, and 7.3 and stands for Cu:Pt atomic ratios) and Pt/SiO2 catalysts.

2. Propane-dehydrogenation Performance Test

1. **Catalyst loading**
    1. Take a 3/8" quartz tube reactor and place a 1 cm layer of quartz wool against the dimple in the middle.
    Caution: Use protective gloves when handling quartz wool, since the fine needles can get imbedded in the skin.
    2. Weigh 40 mg of Pt-0.7Cu/SiO_2 catalyst and 960 mg of the silica for dilution. Mix the particles (1 g total weight) in an empty vial.
    3. Use a plastic funnel to load all the catalyst mixture into the reaction tube. Wipe the outer wall of both tube ends with lint-free wipes to remove any dirt to get a good seal with the O-ring.
    4. Put the tube fittings onto both ends of the quartz reactor tube and attach them to the reactor system equipped with a clamshell furnace.

2. **Leak test and catalyst pretreatment**
    1. Turn on 50 cm^3/min N_2 flow through the tube reactor. After 1 min, close the ball valve on the reactor outlet. Wait for the system pressure to increase to 5 psig. Close the ball valve on the inlet N_2 line to stop N_2 flow and seal the reactor system.
    2. Wait for 1 min and record the pressure read from the gauge. If the pressure drops, open the ball valve on the reactor outlet to release the pressure and re-attach the fittings. If not, first open the ball valve on the reactor outlet to release the pressure before restarting the N_2 flow by turning on the ball valve on the inlet N_2 line to purge the system for 1 min.
    3. Start flowing 50 cm^3/min of 5% H_2/N_2 for catalyst reduction before running a reaction and stop the N_2 flow. Start heating the tube to the reaction temperature of 550 °C, with a rate of 10 °C/min. Wait for 30 min after the furnace reaches the set point and allow the system temperature to stabilize at the target temperature.

3. **Propane dehydrogenation reaction testing**

1. Start the gas chromatograph (GC) in the reactor system and select the proper method for gas component analysis.
    1. Switch the reactor gas flow to a bypass line. Flow 100 cm^3/min of 5% propane/N_2 and 100 cm^3/min of 5% H_2/N_2. Wait for 1 min so that the propane flow stabilizes and inject the bypass flow into GC as a reference sample.
2. Switch the gas flow back to the reactor tube line to start the reaction and record the time.
3. After the reaction runs for 4 min, inject the reactor outlet gas flow (a GC sample) into the GC to get the outlet gas component information. Inject samples every 4 min and run the test until the conversion reaches steady state or the conversion is very low.
4. Use the corresponding peak analysis software to analyze each peak.
    1. Click to select the start and end points of the peak. Use the integrate function to get the peak area. Write down the peak area for the propane (C_3H_8) reactant; the propylene (C_3H_6) product; and the side products, methane (CH_4), ethane (C_2H_4), and ethylene (C_2H_6).
    NOTE: For each injection, a GC pattern with multiple peaks is obtained whose area relates to the number of moles of different gas species.
5. Convert the peak area to the number of moles for each species using the response factor. Determine the propane conversion and propylene selectivity at the time for each sample according to the following formulas:

$$X_{propane} = \frac{n_{propane,in} - n_{propane,out}}{n_{propane,in}}$$

$$S_{propylene} = \frac{n_{propylene,out}}{n_{propane,in} - n_{propane,out}}$$

where $X_{propane}$ is the conversion of propane, $S_{propylene}$ is the propylene selectivity, $n_{propane}$ is the number of moles of propane, and $n_{propylene}$ is the number of moles of propylene.
6. Obtain the initial conversion and selectivity value at t = 0 by extrapolating the measured conversion and selectivity versus time on stream using an exponential fit.

4. **Post-reaction**
    1. Stop heating the reactor by turning off the temperature program. Switch the gas flow to 10 cm^3/min N_2.
    2. Switch the gas chromatograph back to standby method to reduce the flow rate of the carrier gas.
    3. Unload the used catalyst from the quartz fix-bed reactor after cooling to room temperature. Collect the catalyst weight in a designated waste disposal area.

3. Characterization of Catalyst Samples

1. **Scanning Transmission Electron Microscopy**[4,20]
    1. Load the catalyst in a mortar and grind it into less than 100 mesh powder using a pestle.
    2. Disperse about 30 mg of catalyst powder into about 5 mL of isopropyl alcohol in a small vial. Shake the vial for full mixing and then let the vial sit for 5 min to allow for the deposition of the relatively large particles.
    NOTE: The obtained suspension should contain very small particles of supported catalysts.
    3. Place a Au TEM ready grid on an evaporating dish. Heat the dish to 80 °C on a hot plate. Add three drops of the catalyst suspension to the grid.
    NOTE: The isopropyl alcohol will evaporate quickly and leave the catalyst particles on the grid.
    4. Load the grid onto the sample holder for electron microscopy sample imaging.

2. ***In situ* X-ray absorption spectroscopy**[3,4,19,20]
    1. Load the catalyst into a mortar and grind it into less than 100 mesh powder using a pestle. Load the fine powders into a die set and press it with the fingers to form a self-supporting wafer.
    2. Load a ~100 mg sample into the sample holder.
    3. Place the sample holder into a quartz tube reactor and pretreat the sample by reducing it in 50 cm^3/min 3% H_2/He.
    4. After cooling to RT, seal the tube and transfer it to the synchrotron beamline to collect the XAS data.

3. ***In situ* X-ray diffraction** [19,20]
    1. Load the catalyst in a mortar and grind it into less than 100 mesh powder using a pestle.
    2. Press a thin wafer using a standard 7 mm diameter die set.
    NOTE: The die set contains a female piece and top and bottom male pieces.
        1. Attach the bottom male piece to the female part. Load the sample onto the polished surface of the bottom part. Attach the top male piece and transfer the die set to the sample stage of the press. Press with appropriate strength.
    3. Unload the wafer and transfer it to the ceramic cup of the specialized sample stage (see the **Table of Materials**). Seal the stage and fix it on the sample table on the beamline.
    4. Reduce the sample by flowing and ramping the temperature to 550 °C. Collect the *in situ* X-ray diffraction data under 3% H_2/He gas flow at 550 °C and after cooling down to RT[20].

Representative Results

The propylene selectivity versus time for Pt and Pt-Cu catalysts measured at an initial propane conversion of about 20% is presented in **Figure 1A**. Pt catalyst has an initial selectivity of 61%, which increases to about 82% with time on-stream as the catalyst deactivates for 1h. The Pt-0.7Cu catalyst shows a better initial propylene selectivity of 72%. For Pt-2.3Cu and Pt-7.3Cu catalysts, their initial selectivity reach 90% and 96%, respectively, and are maintained with reaction time on-stream. **Figure 1B** shows the change in initial propylene selectivity versus initial propane conversion for the Pt and Pt-7.3Cu catalysts. While the selectivity of the Pt catalysts decreases at higher conversion, the Pt-7.3Cu catalyst retains high propylene selectivity, over 95%, at different propane conversions. When comparing different catalysts, it seems that the catalyst selectivity increases almost linearly with the content of Cu in Pt-Cu catalysts, expressed in atomic percentage, as shown in **Figure 1C**. Increase in the Cu content also improves the turnover rates (TOR) for propane dehydrogenation. **Figure 1D** displace the close linear relationship between the TOR and the catalyst atomic ratio of Cu to Pt. The carbon balance is close to 100% during all reaction tests, although minor coke formation occurs throughout the reaction.

STEM images were collected for monometallic Pt and three Pt-Cu catalysts with different metal loadings and Cu:Pt ratios, as confirmed by atomic absorption spectroscopy. The particle sizes of all catalysts determined by STEM imaging are between 2 and 3 nm. **Figure 2A** shows an STEM image of a Pt-2.3Cu catalyst, which is typical of the other samples. The average particle size of the sample is determined to be 2.2 nm, with a standard deviation of 0.4 nm. For Pt-0.7Cu and Pt-7.3Cu, the obtained STEM particle sizes are 2.5 ±0.4 nm and 2.1 ±0.4 nm. *In situ* X-ray absorption near edge spectroscopy at both the Pt and Cu edges have been done to determine the valence states of Pt and Cu under conditions similar to the reaction environment. Both Pt and Cu are found to be fully reduced to the metallic state. The magnitude of the k^2 weighted Fourier transform of extended X-ray absorption fine structure (EXAFS) spectra for Pt and Pt-Cu catalysts at the Pt L_{III} edge are shown in **Figure 2B**. At the Pt L_{III} edge, the Pt catalyst shows a three-peak pattern typical of Pt-Pt scattering. For Pt-0.7Cu, the peak position of three-peak pattern is shifted to lower R, suggesting the interference of the Pt-Pt scattering by a second Pt-Cu scattering with a shorter bond distance. The EXAFS spectra of Pt-2.3Cu and Pt-7.3Cu, which contain a relative high amount of Cu, show only one peak, typical of Pt-Cu metal scattering. The change of the scattering pattern with increasing Cu:Pt atomic ratio suggests the formation of bimetallic nanoparticles with increasing Cu content percentage. **Figure 2C** displays a background-subtracted *in situ* synchrotron X-ray diffraction (XRD) pattern of Pt and Pt-Cu catalysts and the corresponding simulated XRD pattern of the identified Pt-Cu phases. No superlattice diffraction is found, and the composition of the Pt-Cu catalysts is different from the ideal composition of ordered alloys, indicating that Pt and Cu form a solid solution structure in the Pt-Cu catalysts. The diffraction peaks of the catalysts with increasing Cu:Pt atomic ratio shift to higher angles, and their normalized intensities decrease, all confirming that the solid solution becomes richer in Cu. The composition of the solid solution is calculated from the diffraction pattern using Bragg's Law and Vegard's Law.

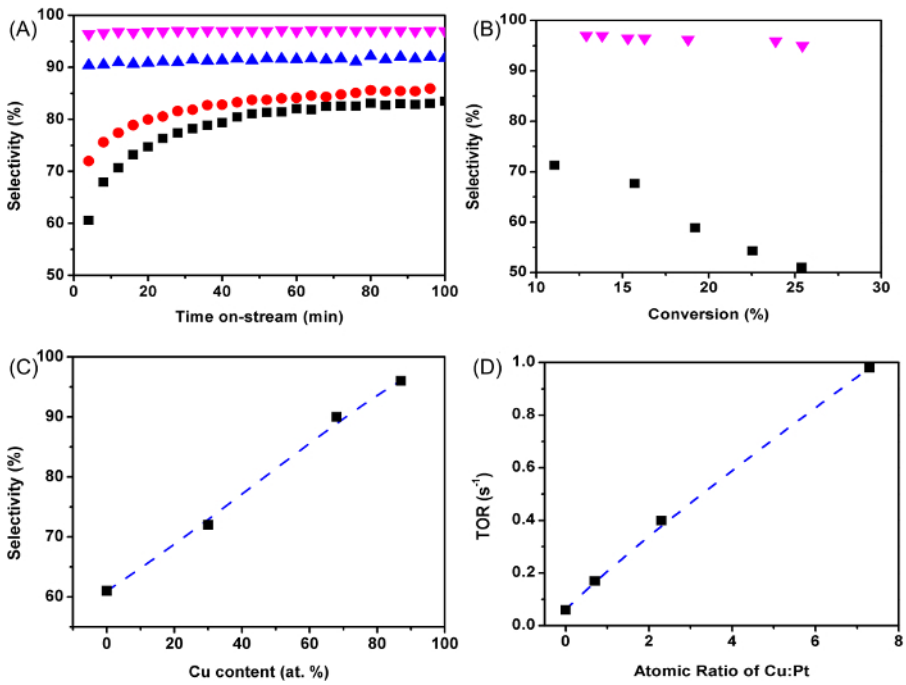

Figure 1: Propane-dehydrogenation Performance of Pt and Pt-Cu Catalysts. (**A**) Propylene selectivity versus the time measured at 550 °C for the Pt (black squares), Pt-0.7Cu (red circles), Pt-2.3Cu (blue triangles), and Pt-7.3Cu (magenta down triangles) catalysts. (**B**) Propylene selectivity versus propane conversion measured at 550 °C for the Pt (black squares) and Pt-7.3Cu (magenta down triangles) catalysts. (**C**) Dehydrogenation selectivity versus Cu content in atomic percentage. (**D**) Turnover rate versus the Cu:Pt atomic ratio of each catalyst Please click here to view a larger version of this figure.

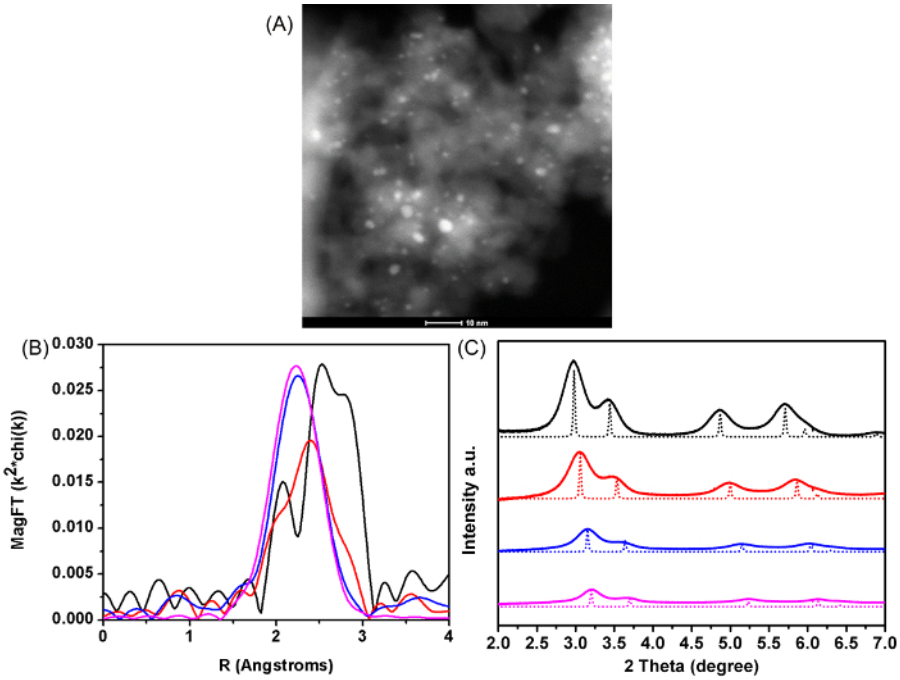

Figure 2: Structures of Pt and Pt-Cu Catalysts. (**A**) STEM high-angle annular dark field (HAADF) image of the Pt-2.3Cu catalyst. (**B**) Pt L_{III} edge magnitude of the Fourier transform of the EXAFS of Pt (black), Pt-0.7Cu (red), Pt-2.3Cu (blue), and Pt-7.3Cu (magenta). (**C**) Background-subtracted *in situ* XRD pattern of: Pt (black, solid), Pt-0.7Cu (red, solid), Pt-2.3Cu (blue, solid), and Pt-7.3Cu (magenta, solid) compared with the simulated XRD pattern of: bulk FCC Pt (black, dotted), $Pt_{0.70}Cu_{0.30}$ (red, dotted), $Pt_{0.32}Cu_{0.68}$ (blue, dotted), and $Pt_{0.13}Cu_{0.87}$ (magenta, dotted), respectively. Please click here to view a larger version of this figure.

Discussion

The Pt-Cu catalysts prepared in this work contain uniform nanoparticles around 2 nm in size, similar to heterogeneous catalysts qualified for industrial application. All the Pt and Cu precursors form bimetallic structures, as opposed to separate monometallic particles. This bimetallic interaction and small particle size are realized by careful control over the synthesis procedures. The impregnation process makes use of the Strong Electrostatic Adsorption (SEA) between metal ions and the surface of certain oxide supports[21]. Oxide materials such as silica have hydroxyl groups on the surface, which can be protonated or deprotonated in a solution depending on the pH. Silica has a characteristic Point of Zero Charge (PZC) around pH = 4[22], which means that the surface is electronically neutral at this pH. The oxide surface would be deprotonated and adsorb cations if the pH of the solution goes above its PZC, whereas at Ph values below PZC, it would protonate and adsorb anions. By adjusting the pH of the precursor solution to greater than 10 by adding ammonia, as shown in step 1.1.3, the solution is under basic conditions, so the silica hydroxyl groups are sufficiently deprotonated and are able to strongly adsorb cations such as platinum tetraammine $[(NH_3)_4Pt]^{2+}$ and copper tetraammine complexes $[(NH_3)_4Cu]^{2+}$. The electronic attraction between the cations and the deprotonated hydroxyl groups anchors the precursor on the catalyst, and the repulsion between the cations aids in their dispersion, both of which help to prevent the agglomeration of the metal species upon calcination and reduction. The impregnation processes of the two different metal precursors are conducted in parallel. Compared with sequential impregnation, the co-impregnation method ensures the uniform distribution of the two metal precursors in the solution to maximize their mixing. The obtained supported Pt-Cu catalysts, therefore, show strong bimetallic interaction, and no monometallic particles are formed. The impregnation is also carried out in incipient wetness, which optimizes the dispersion of the precursor solution in the pores of the support oxide by capillary effect. The impregnated Pt-Cu catalysts are calcined at 250 °C to remove the ligand attached to the metals while minimizing the growth of the oxide clusters. The calcination temperature of the impregnated metal precursors has been shown to affect the size of the reduced metal nanoparticles[23,24].

For Pt on silica, the particle size increases with increasing temperature, and temperatures near 250 °C are necessary to give small nanoparticles. The optimum calcination temperature is different for other metals and supports. When reducing the Pt-Cu catalysts, a high H_2 flow rate and a slow ramping rate are used at around the reduction temperature of Pt to quickly remove the water formed during reduction, thus suppressing the growth of the metal nucleus. The goal is to raise the temperature to just below the point where rapid reduction occurs to slowly reduce the metal oxide while quickly removing the water formed during reduction. Thus, it is important to approach the reduction slowly and to hold at that temperature for sufficient time while removing the water under high flow. Once reduced, the temperature can be raised quickly to the reaction temperature. It is important to reduce the entirety of the catalysts to the highest temperature they will be exposed to during the reaction condition so that they do not go through additional sintering when the reaction is running. Once reduced, exposure to air at room temperature will oxidize the particle surface but not the entire particle. Further rereduction will give almost the same particle size. Thus, if the entire particle is reduced, the size will be fixed for every analysis (*i.e.* the particle size for kinetics, infrared (IR) spectroscopy, XAS, XRD, etc. will be identical). The whole catalyst synthesis protocol is also applicable to the preparation of other metal catalysts used in various applications[25] to obtain strong bimetallic interactions, and smaller or larger particle sizes can be obtained via minor modification of the protocol.

In situ synchrotron XRD was performed to investigate the crystal structure of the 2-nm Pt-Cu nanoparticles. For supported nanoparticles below 3 nm in size, diffraction is very challenging to measure using laboratory instrument[19]. The diffraction peaks are strongly broadened and very low in intensity due to the limited repetition of unit cells. In addition, the metal loading of supported metal catalysts is typically low (≤5%), which

further lowers the diffraction signal. Moreover, a large fraction of the atoms is at the particle surface (close to 50% for 2 nm nanoparticles) and is oxidized when measured in air. Therefore, to obtain meaningful structural information, the diffraction must be collected *in situ* using high-flux X-ray, typically only available with a synchrotron. In this case, the X-ray diffraction patterns are first measured under 3% H_2/He at 550 °C after reduction and then at room temperature in the same atmosphere after cooling. The diffraction signals from the metals in the catalysts are isolated from the raw data by subtracting the SiO_2 support and sample cell diffraction using the patterns taken at the same condition. The two patterns show the same phase, indicating the unchanged crystal structure of the catalysts at the two different temperatures.

In situ XRD and XAS suggest that, for the Pt-Cu catalysts with increasing Cu:Pt atomic ratio, a series of substitutional solid-solution structure with increasing Cu content percentage are formed. In a solid-solution structure, Pt and Cu atoms are randomly distributed; therefore, the Pt atoms are not necessarily bonded each other. However, the isolation of Pt atoms by Cu is realized at a high Cu:Pt ratio, and the extent of the Pt site isolation improves as the atomic percentage of Cu increases. This change in the structure of active sites translates into improvements in the PDH selectivity of the Pt-Cu catalysts (**Figure 1C**), confirming the relationship between site isolation and high dehydrogenation selectivity. For the Pt-7.3Cu catalyst with the highest Cu content, almost all the Pt atoms are isolated, as shown by EXAFS. As a result, the selectivity of this catalyst remains high (close to 100%) at varied initial conversion. In addition to changes in the selectivity, improved site isolation also introduces an increasing amount of Cu neighbors bonded to the Pt atoms and electronically modifies the Pt active sites. As a result, the turnover rate of the catalyst for PDH also continues to increase with the atomic ratio of Cu:Pt (**Figure 1D**). A TOR of 0.98 s^{-1} for Pt-7.3Cu is 16 times higher than the TOR of 0.06 s^{-1} for monometallic Pt and is also higher than the typical TOR values (0.1-0.5 s^{-1}) of Pt-Sn catalysts under similar reaction conditions[1].

In the manuscript, we have demonstrated a convenient method for the synthesis of bimetallic Pt-Cu catalysts, as well as performance tests for propane dehydrogenation and characterization. The catalyst forms a substitutional solid-solution structure, with a small and uniform particle size around 2 nm, which is realized by careful control over the impregnation, calcination, and reduction steps during catalyst preparation and is identified by advanced *in situ* synchrotron techniques. The catalyst performance continuously improves with increasing Cu:Pt atomic ratio.

Disclosures

The authors have nothing to disclose.

Acknowledgements

This work was supported by the School of Chemical Engineering, Purdue University. Use of the Advanced Photon Source was supported by the U.S. Department of Energy, Office of Basic Energy Sciences, under contract no. DE-AC02-06CH11357. MRCAT operations, beamline 10-BM are supported by the Department of Energy and the MRCAT member institutions. The authors also acknowledge the use of beamline 11-ID-C. We thank Evan Wegener for experimental assistance with the XAS.

References

1. Sattler, J. J., Ruiz-Martinez, J., Santillan-Jimenez, E., Weckhuysen, B. M. Catalytic dehydrogenation of light alkanes on metals and metal oxides. *Chem. Rev.* **114** (20), 10613-10653 (2014).
2. Childers, D. J. *et al.* Modifying structure-sensitive reactions by addition of Zn to Pd. *J Catal.* **318**, 75-84 (2014).
3. Gallagher, J. R. *et al.* Structural evolution of an intermetallic Pd-Zn catalyst selective for propane dehydrogenation. *Phys. Chem. Chem. Phys.* **17**, 28144-28153 (2015).
4. Wu, Z. *et al.* Pd-In intermetallic alloy nanoparticles: highly selective ethane dehydrogenation catalysts. *Catal Sci Technol.* **6** (18), 6965-6976 (2016).
5. Siddiqi, G., Sun, P., Galvita, V., Bell, A. T. Catalyst performance of novel Pt/Mg (Ga)(Al) O catalysts for alkane dehydrogenation. *J Catal.* **274** (2), 200-206 (2010).
6. Passos, F. B., Aranda, D. A., Schmal, M. Characterization and catalytic activity of bimetallic Pt-In/Al 2 O 3 and Pt-Sn/Al 2 O 3 catalysts. *J Catal.* **178** (2), 478-488 (1998).
7. Virnovskaia, A., Morandi, S., Rytter, E., Ghiotti, G., Olsbye, U. Characterization of Pt, Sn/Mg (Al) O catalysts for light alkane dehydrogenation by FT-IR spectroscopy and catalytic measurements. *J Phys Chem C.* **111** (40), 14732-14742 (2007).
8. Jablonski, E., Castro, A., Scelza, O., De Miguel, S. Effect of Ga addition to Pt/Al 2 O 3 on the activity, selectivity and deactivation in the propane dehydrogenation. *Appl Catal A.* **183** (1), 189-198 (1999).
9. Galvita, V., Siddiqi, G., Sun, P., Bell, A. T. Ethane dehydrogenation on Pt/Mg (Al) O and PtSn/Mg (Al) O catalysts. *J Catal.* **271** (2), 209-219 (2010).
10. Shen, J., Hill, J. M., Watwe, R. M., Spiewak, B. E., Dumesic, J. A. Microcalorimetric, infrared spectroscopic, and DFT studies of ethylene adsorption on Pt/SiO2 and Pt-Sn/SiO2 catalysts. *J Phys Chem B.* **103** (19), 3923-3934 (1999).
11. Silvestre-Albero, J. *et al.* Microcalorimetric, reaction kinetics and DFT studies of Pt-Zn/X-zeolite for isobutane dehydrogenation. *Catal Lett.* **74** (1-2), 17-25 (2001).
12. Sun, P., Siddiqi, G., Vining, W. C., Chi, M., Bell, A. T. Novel Pt/Mg (In)(Al) O catalysts for ethane and propane dehydrogenation. *J Catal.* **282** (1), 165-174 (2011).
13. Sun, P., Siddiqi, G., Chi, M., Bell, A. T. Synthesis and characterization of a new catalyst Pt/Mg (Ga)(Al) O for alkane dehydrogenation. *J Catal.* **274** (2), 192-199 (2010).
14. Okamoto, H. *Phase diagrams for binary alloys. Desk handbook.* ASM International, Member/Customer Service Center. Materials Park, OH 44073-0002, USA. 828. (2000).
15. Hamid, S. B. D.-A., Lambert, D., Derouane, E. G. Dehydroisomerisation of n-butane over (Pt, Cu)/H-TON catalysts. *Catal Today.* **63** (2), 237-247 (2000).

16. Veldurthi, S., Shin, C.-H., Joo, O.-S., Jung, K.-D. Promotional effects of Cu on Pt/Al 2 O 3 and Pd/Al 2 O 3 catalysts during n-butane dehydrogenation. *Catal Today.* **185** (1), 88-93 (2012).
17. Han, Z. *et al.* Propane dehydrogenation over Pt-Cu bimetallic catalysts: the nature of coke deposition and the role of copper. *Nanoscale.* **6** (17), 10000-10008 (2014).
18. Komatsu, T., Tamura, A. Pt 3 Co and PtCu intermetallic compounds: promising catalysts for preferential oxidation of CO in excess hydrogen. *J Catal.* **258** (2), 306-314 (2008).
19. Gallagher, J. R. *et al.* In situ diffraction of highly dispersed supported platinum nanoparticles. *Catal Sci Technol.* **4** (9), 3053-3063 (2014).
20. Ma, Z., Wu, Z., Miller, J. T. Effect of Cu content on the bimetallic Pt-Cu catalysts for propane dehydrogenation. *Catal Struct React.* **3** (1-2), 43-53 (2017).
21. Richards, R. *Surface and nanomolecular catalysis.* CRC Press. (2006).
22. Jiao, L., Regalbuto, J. R. The synthesis of highly dispersed noble and base metals on silica via strong electrostatic adsorption: I. Amorphous silica. *J Catal.* **260** (2), 329-341 (2008).
23. Miller, J. T., Schreier, M., Kropf, A. J., Regalbuto, J. R. A fundamental study of platinum tetraammine impregnation of silica: 2. The effect of method of preparation, loading, and calcination temperature on (reduced) particle size. *J Catal.* **225** (1), 203-212 (2004).
24. Wei, H. *et al.* Selective hydrogenation of acrolein on supported silver catalysts: A kinetics study of particle size effects. *J Catal.* **298**, 18-26 (2013).
25. Ertl, G., Knözinger, H., Schüth, F., Weitkamp, J. *Handbook of heterogeneous catalysis: 8 volumes.* Wiley-vch. (2008).

